ChemPubSoc Europe

DOI: 10.1002/cbic.201300770

Methyl Yellow: A Potential Drug Scaffold for Parkinson's Disease

Werner J. Geldenhuys,*[a] Akiko Kochi,[b] Li Lin,[a] Vijaykumar Sutariya,[c] Dean E. Dluzen,[a] Cornelis J. Van der Schyf,[d] and Mi Hee Lim*[b, e]

Parkinson's disease (PD) is an age-related neurodegenerative disease affecting movement. To date, there are no currently available therapeutic agents which can prevent or slow disease progression. Here, we evaluated an azobenzene derivative, methyl yellow (MY), as a potential drug scaffold for PD; its inhibitory activity toward monoamine oxidase B (MAO-B) as well as drug-like properties were investigated. The inhibitory effect of MY on MAO activity was determined by a MAO enzyme inhibition assay. In addition, the in vitro properties of MY as a drug candidate (e.g., blood–brain barrier (BBB) permeability, serum albumin binding, drug efflux through P-glycoprotein (P-gp), drug metabolism by P450, and mitochondrial toxicity) were examined. In vivo effectiveness of MY was also evaluated in the 1-methyl-4-phenyl-1,2,3,6-tetrahydropyridine (MPTP) Parkinsonian mouse model. MY selectively inhibited MAO-B in a dose-dependent and reversible manner. MY was BBB-permeable, bound relatively weakly to serum albumin, was an unlikely substrate for both systems of P-gp and P450, and did not cause mitochondrial toxicity. Results from the MPTP Parkinsonian mouse model indicated that, upon treatment with MY, neurotoxicity induced by MPTP was mitigated. Investigations of MY demonstrate its inhibitory activity toward MAO-B, compliant properties for drug consideration, and its neuroprotective capability in the MPTP Parkinsonian mouse model. These data provide insights into potential use, optimization, and new design of azobenzene derivatives for PD treatment.

Introduction

Idiopathic Parkinson's disease (PD) is an age-related neurodegenerative disorder that largely affects patients over the age of 65.[1] In younger patients, the disease has been shown to be genetically linked.[2] PD largely affects the dopaminergic pathways, which ultimately leads to loss of fine motor control. The loss of these neurons in the substantia nigra yields the classical motor-associated symptoms of resting tremor, bradykinesia, and balance impairment.[3] Later stages of the disease are also correlated with other neurological symptoms, such as dementia and depression.[4] The exact etiology of PD is still unknown, although it is suggested that environmental factors, such as pesticide exposure, might play a large role.[5]

One of the causes attributed to the cell death observed in brains of PD patients is the formation of reactive oxygen species (ROS). These ROS originate from several sources, of which the activity of monoamine oxidases A and B (MAO-A and MAO-B), bound on the outer membrane of mitochondria, has been implicated as the major source of ROS production.[6] An increase in MAO-B enzyme levels in aging patients has been observed with an increase in loss of dopaminergic neurons, and the resulting presence of ROS has been indicated as one of the main apoptotic inducers in neuronal cell death.[6b]

MAO-B inhibitors have been historically used as part of the pharmacotherapy of PD, in addition to the mainstay therapy of L-DOPA and a peripheral decarboxylase inhibitor.[7] In addition to providing symptomatic relief through inhibition of dopamine metabolism,[8] several lines of evidence have suggested that MAO-B inhibitors are neuroprotective.[9] The significant role of ROS through MAO-B in PD has led to the development of several compounds that inhibit MAO-B.[7b,10] Multifunctional MAO-B compounds (containing inhibitory as well as neuroprotective activity) would be useful for treatment if they were nontoxic and able to penetrate the blood–brain barrier (BBB), among other favorable drug-like characteristics. With the focus on these requirements, we initiated a search for compounds similar to the stilbene framework, for which we previously showed MAO-B inhibitory activity.[11] The well-studied representative of this class, resveratrol, has been shown to have several beneficial effects on mitochondrial dysfunction[12] and in PD

[a] Dr. W. J. Geldenhuys, L. Lin, Dr. D. E. Dluzen
Neurotherapeutics Emphasis Group
Department of Pharmaceutical Sciences
Northeast Ohio Medial University (NEOMED), College of Pharmacy
4209 State Route 44, Rootstown, OH 44272 (USA)
E-mail: wgeldenh@neomed.edu

[b] Dr. A. Kochi, Prof. M. H. Lim
Department of Chemistry and Life Sciences Institute, University of Michigan
210 Washtenaw Avenue, Ann Arbor, MI 48109 (USA)

[c] Dr. V. Sutariya
Department of Pharmaceutical Sciences, University of South Florida
12901 Bruce B. Downs Blvd., MDC 30, Tampa, FL 33612 (USA)

[d] Prof. C. J. Van der Schyf
Department of Pharmaceutical Sciences, Idaho State University
921 S. 8th Avenue, Pocatello, ID 83209 (USA)

[e] Prof. M. H. Lim
Department of Chemistry
Ulsan National Institute of Science and Technology (UNIST)
50 UNIST-gil, Eonyan-eup, Ulju-gun, Ulsan 689-798 (Republic of Korea)
E-mail: mhlim@unist.ac.kr

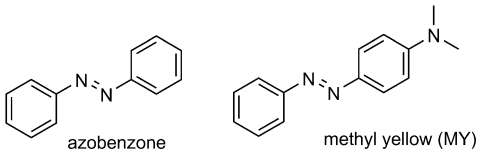

Scheme 1. Structures of azobenzene ((*E*)-1,2-diphenyldiazene) and methyl yellow (MY, (*E*)-*N*,*N*-dimethyl-4-(phenyldiazenyl)aniline).

models[,13c] and, as reviewed elsewhere, has led to the development of several published compound sets with CNS activity.[14] Herein, we report the MAO-B inhibitory activity of two small molecules, azobenzene and methyl yellow (MY; Scheme 1), and further investigation of MY as a potential drug candidate through the evaluation of its BBB permeability, drug efficacy (i.e., serum albumin binding, elimination through drug efflux/metabolism), and neuroprotection in a 1-methyl-4-phenyl-1,2,3,6-tetrahydropyridine (MPTP) Parkinsonian mouse model.

Results

MAO inhibition

The activity of azobenzene and MY (Scheme 1) toward MAO inhibition was determined by using recombinant human enzymes, as previously described, with minor modifications.[15] As seen in Table 1, both azobenzene and MY showed abilities to inhibit the activity of both MAO-A and MAO-B; they appeared to be selective toward MAO-B over MAO-A to some extent. MY in particular, was observed to be a potent, relatively selective MAO-B inhibitor (IC_{50} = ca. 15 nM and 5 μM for MAO-B and MAO-A, respectively), compared to known inhibitors such as rasagiline (IC_{50} = 14 nM for MAO-B) and safinamide (IC_{50} = 80 nM for MAO-B).[16] In addition, based on time course and Michaelis–Menten kinetic studies (Figures 1 and 2), MY could be classified as a reversible inhibitor that acts in a dose-dependent manner.

Table 1. Inhibitory activity of azobenzene and MY toward MAO enzyme activity in 96-well plate format. Enzyme activity was measured by fluorescence following the conversion of nonfluorescent kynuramine to its fluorescent product.

Compound	IC_{50} [μM] MAO-A	MAO-B
azobenzene	22.9 ± 0.1	2.66 ± 0.054
MY	4.64 ± 0.05	0.0146 ± 0.017
zonisamide[a]		22.61 ± 1.26

[a] Positive control.[39]

Molecular docking

In order to gain insight into the binding mode of MY into MAO-B, ligand docking studies were conducted with MOE 2011.10, by using a protein structure of MAO-B that was previously determined with (*S*)-(+)-2-[4-(fluorobenzyloxy-amino)propionamide] cocrystallized with the gating residue Ile199 in the open position (PDB ID: 2V5Z)[16b] (Figure 4). MY was observed to be oriented with the dimethylamino moiety toward the flavin adenine dinucleotide (FAD), with the terminal aromatic ring spanning the entrance and substrate cavities (Figure 3 A). Potential interaction with the gate residues (Phe168, Leu171, Ile199, and Tyr326) might have resulted in MY residing in both cavities (Figure 3 B).

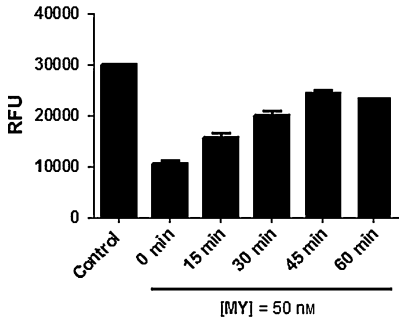

Figure 1. Time–effect experiments on the catalytic activity of MAO-B in the presence of MY (50 nM). Time points indicate the preincubation of MAO-B with MY. Enzymatic activity was measured after 20 min incubation with substrate kynuramine (λ_{ex} = 310 nm; λ_{em} = 380 nm). Data are shown as mean ± SD, where n = 8.

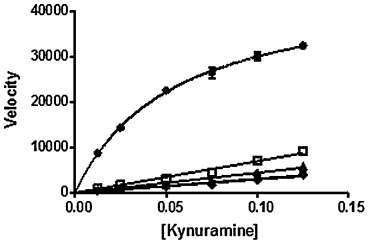

Figure 2. Effect of MY on the maximal rate of MAO-B activity. The MAO-B catalytic activity of kynuramine, used as a substrate, in the absence and presence of 0 (●), 100 (□), 200 (▲), 300 (▼), and 400 nM (◆) MY was determined as described in the Experimental Section.

Brain uptake studies

The ability of MY to passively diffuse through the BBB was first evaluated by employing a parallel artificial membrane permeability assay (PAMPA) assay.[17] The permeability value ($-\log P_e$) for MY was measured as −4.26 ± 0.62, compared to the BBB-permeable compound propranolol ($-\log P_e$ = −4.17 ± 0.39), thus suggesting that MY could possibly permeate the BBB. Moving forward, the potential brain uptake of MY was further evaluated in vivo by determining the concentration of the compound after treatment in the brain of C57BL/6 mice. MY was injected intraperitoneally at 1 mg mg^{-1}, and its concentration in the brain was analyzed after 1 h by HPLC (Figure S1). These results indicated that MY could enter the brain to accumulate at a concentration of ca. 500 nM, which was identified through a standard curve (r^2 = 0.999).

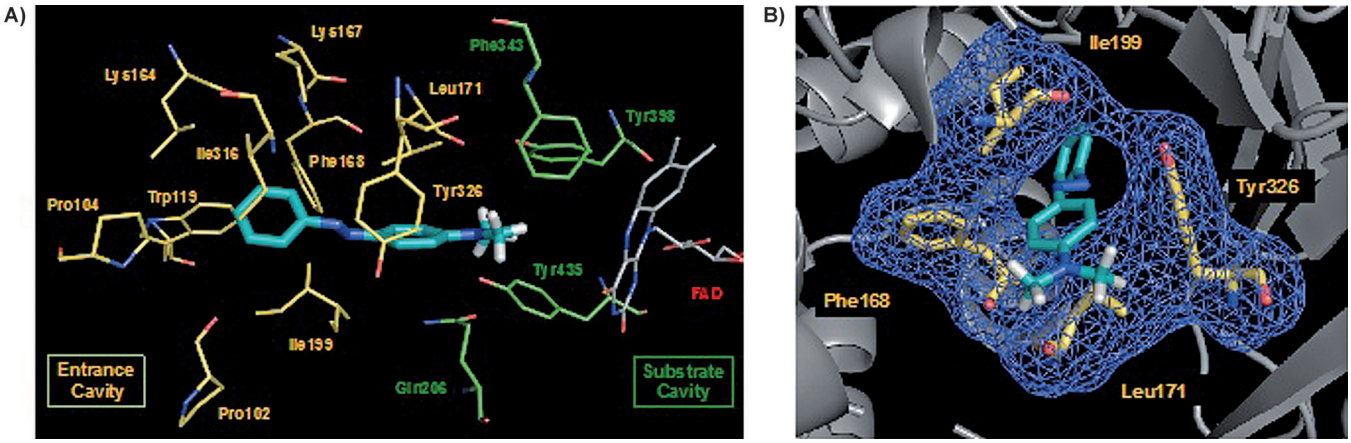

Figure 3. Docking studies of MY with MAO-B. The compound was superimposed into the active site of MAO-B bound to the inhibitor safinamide in the crystal structure (PDB ID: 2V5Z). In the figure, nitrogen, hydrogen, and oxygen atoms are coded as blue, white, and red, respectively. A) Residues within 5 Å surrounding MY situated at the active site of MAO-B (some omitted for clarity) are divided into entrance cavity (yellow) and substrate cavity (green). The flavin adenine dinucleotide (FAD) cofactor (gray) is positioned at the outer boundary of the substrate cavity. B) Surface representation of MY, which is surrounded by the four gate residues and occupies both the entrance and substrate cavities.

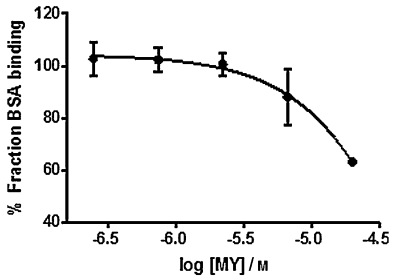

Figure 4. Binding of MY to bovine serum albumin (BSA). Serial dilutions of MY were treated with BSA (final concentration = 7.5 μM), and fluorescence quenching was monitored at λ_{ex} = 280 nm; λ_{em} = 340 nm.

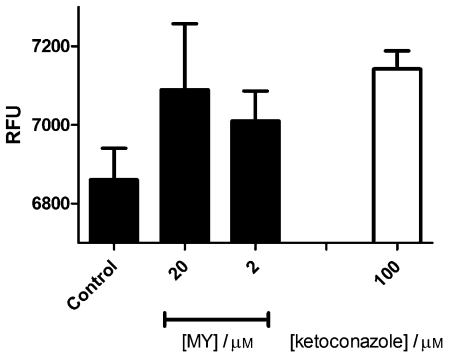

Figure 5. Effect of MY on P450 metabolism in crude liver microsomes. Metabolic activity of P450 was determined by measurement of NADPH fluorescence (λ_{ex} = 340 nm; λ_{em} = 450 nm) in the presence of A) ketoconazole or B) MY.

Serum albumin binding

The effect of MY on bovine serum albumin (BSA) binding was investigated by a high-throughput screening (HTS) assay. This assay measures the degree of fluorescence quenching that indicates possible ligand binding to either the Sudlow I or II pocket in BSA.[17a,18] As indicated in Figure 4, MY was observed to have relatively weak binding toward BSA; binding to BSA only occurred at higher concentrations (> 1 mM), and 50% binding occurred at approximately 100 μM.

P450 enzyme metabolism

The metabolism of MY was evaluated by using crude murine liver microsomes (Figure 5). The activity of P450 was determined by measuring the use of nicotinamide adenine dinucleotide phosphate (NADPH) by the enzyme; a decrease in the fluorescence of NADPH upon addition of compound indicates metabolic activity.[19] As a positive control, ketoconazole, a known CYP3A4/5 inhibitor, was used to show that metabolic activity of P450 decreased upon increasing concentrations of compound[20] (Figure 5). With the addition of MY, a similar trend was observed in which the metabolic activity of P450 was reduced (Figure 5), thus implying that this compound would be an unlikely substrate for P450.

ATPase activity of P-glycoprotein

As P-gp plays an integral role in efflux of xenobiotics from the brain,[21] a P-gp ATPase assay[22] was performed in order to identify whether MY is a possible substrate for P-gp. As shown in Figure 7, MY does not seem to act as a substrate for P-gp, in comparison to verapamil, a known P-gp substrate.[23]

Mitochondrial membrane potential

In order to assess whether MY could be used for in vivo studies, mitochondrial toxicity of MY was measured by using an HTS detection assay[24] (Figure 7). The membrane potential was compared against trifluorocarbonylcyanide phenylhydrazone (FCCP), a chemical uncoupler of electron transport and oxidative phosphorylation.[25] FCCP was observed to affect the mem-

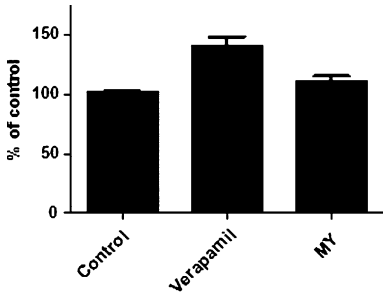

Figure 6. Effect of MY on ATPase activity of P-glycoprotein (P-gp). Recombinant human P-gp was treated with a solution of drug or vehicle. ATPase activity was initiated upon addition of reaction buffer and was determined by the detection of luminescence generated by an ATP-dependent firefly luciferase reaction.

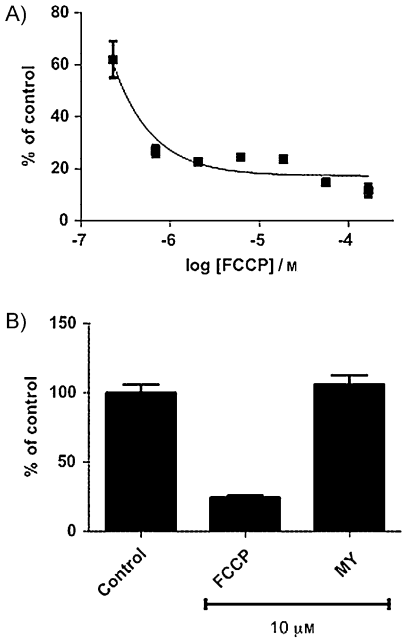

Figure 7. Evaluation of mitochondria membrane potential in the presence of varying concentrations of A) trifluorocarbonylcyanide phenylhydrazone (FCCP) or B) a single concentration of FCCP and MY (10 μM).

brane potential in a dose-dependent manner (Figure 7 A); however, treatment with MY did not indicate a loss in membrane potential (Figure 7 B).

Dopamine depletion

The potential of MY as a possible neuroprotective agent was examined in a Parkinsonian mouse model induced by MPTP, a neurotoxin precursor to MPP^+, which causes permanent symptoms of PD.[26] The effect of MY upon striatal dopamine (DA) loss in the presence of MPTP was evaluated. As observed in Figure 8, the level of DA was significantly elevated by treatment with MY in the presence of MPTP. This result suggests that MY could serve as an effective agent for neuroprotection in PD.

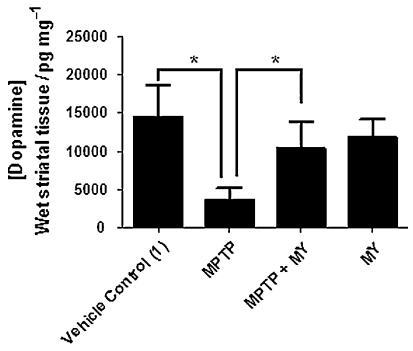

Figure 8. Effect of MY toward MPTP-induced striatal dopamine depletion in the MPTP Parkinsonian mouse model. The experimental details are described in the Experimental Section. Each bar represents mean ± SD, where $n = 3–4$ mice per group. * Statistical significance $P < 0.05$.

Tyrosine hydroxylase expression

The effect of MY against the loss of tyrosine hydroxylase (TH) expression in the MPTP mouse model was assessed. The level of TH was observed to be unaffected in MY-treated mice, compared to that in analogous, compound-free mice (Figure 9). Furthermore, upon administration of MY, TH concentration was not shown to be reduced, even in the presence of MPTP, which significantly decreased protein expression by itself (Figure 9).

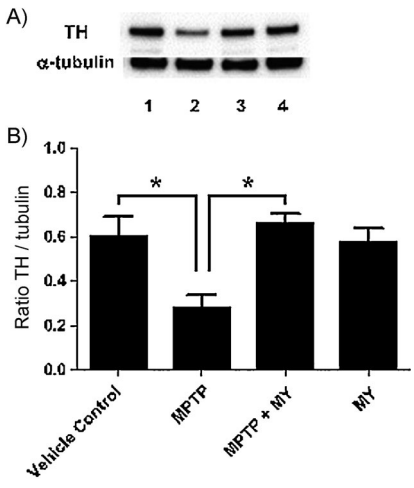

Figure 9. Western blot analysis of striatal tyrosine hydroxylase (TH) protein expression levels. Groups are 1) vehicle control (DMSO); 2) mice treated with MPTP; 3) mice treated with both MPTP and MY; 4) mice treated with MY only. Each bar represents mean ± SD, where $n = 3–4$ mice per group. * Statistical significance $P < 0.05$.

Discussion

MY, an azobenzene derivative with a backbone similar to that of stilbene, was evaluated as a potential MAO-B inhibitor for use in PD treatment. Ligands with the stilbene framework have been previously shown to have MAO-B inhibitory activity.[11] Moreover, stilbene has been highlighted lately, due to the

myriad of activities demonstrated by resveratrol.[27] Although resveratrol itself has been shown to be largely devoid of MAO inhibitory activity,[28] we were able to establish MAO-B inhibition upon addition of a compound containing the dimethylamino group on the stilbene framework. MY containing a dimethylamino group was observed to be a more potent MAO-B inhibitor, showing an IC_{50} value approximately 15 nM lower than that of azobenzene. In addition, MY presented relative selectivity (ca. 250-fold) toward MAO-B over MAO-A. Here, MY showed similar activity to that reported for other dyes .[30] For instance, methylene blue has been shown to inhibit MAO-B and was shown to be neuroprotective in an MPTP toxin model.[28] Additionally, the metabolite of methylene blue, azure B, was shown to be a much more potent MAO-B inhibitor.[30,31] These dyes, therefore, might be a rich source of novel MAO-B inhibitors.

In light of MY showing a favorable capability to inhibit MAO-B, we further characterized the compound as a possible drug scaffold. A PAMPA assay was first performed to predict brain distribution potential of MY. The permeability value of MY suggests that the compound could possibly pass through the BBB and be distributed into the CNS.[32] Assessing initial permeability is critical, due to the fact that 98% of CNS drug clinical trial failures are attributed to poor BBB penetration.[33] Along with the PAMPA study, initial brain uptake of MY was investigated in vivo, accumulation of compound at 500 nM 1 h post-injection into the brain of C5BL/6 mice was indicated, several-fold higher than the IC_{50} required for MAO-B inhibition (Table 1). Additionally, whether or not the P-gp efflux pump plays a significant role in the removal of MY from the brain, as it does with other drugs,[21] was evaluated. As seen in Figure 6, MY did not act as a substrate for P-gp, as evidenced by the lack of increased ATP usage associated with an increase in P-gp activity. This suggests that removal from the brain upon uptake might occasionally occur. Verapamil was used as positive control to indicate the effect of a known substrate in our assay.

Potential drug clearance occurring outside the brain was analyzed. P450 liver enzymes are involved in detoxification,[34] and in order to determine whether MY could be a substrate for P450, the metabolism of MY was evaluated by using crude murine liver microsomes. MY was observed to be an unlikely substrate for liver P450, implying that when dosed in vivo, clearance from the bloodstream could be low (Figure 5). Ketoconazole, a known inhibitor of liver P450 enzymes, is shown as a positive control. Moreover, MY was shown to bind weakly to BSA (Figure 4); the concentration of drug in the blood might therefore be close to therapeutically relevant levels without the need to increase the dosage.

PD has been associated with mitochondrial dysfunction.[35] The oxidative stress from dysfunctional mitochondria, as well as from the inhibition of mitochondrial complex I by $MPP+$, led us to evaluate the mitochondrial toxicity potential of MY in vitro. MY did not alter the mitochondrial membrane potential, indicating that it was safe for use in preclinical models of PD in vivo. The possible neuroprotective role of MY in vivo (i.e., the MPTP Parkinsonian mouse model) was further evaluated. MPTP is a protoxin that is converted to its toxic pyridinium metabolite MPP^+ in astroglia, whereupon it is taken up in the presynaptic terminal through the dopamine transporter.[36] MPP^+ itself is a complex I inhibitor that leads to increased generation of ROS and induces severe dopaminergic cell death.[26b] Upon injection of MY as a pretreatment before MPTP treatment, the mice were protected against the neurotoxin, as evidenced by the mitigation of striatal DA loss as compared to mice treated with MPTP alone (Figure 8). Protection against DA loss was also corroborated by the level of TH expression, which is responsible for catalyzing conversion of the amino acid L-tyrosine to L-3,4-dihydroxyphenylalanine (L-DOPA), the precursor to dopamine.[37] With MY treatment, consistent expression of TH was observed even in the presence of MPTP, which suppresses TH levels, suggesting that MY might aid in increasing DA levels that are highly reduced in PD-afflicted brains (Figure 9). Taking into consideration the fact that MY was shown to be an MAO-B inhibitor, the mechanism of protection in our in vivo model appeared to be the prevention of a neurotoxic pathway: transformation of MPTP to MPP^+. As neurodegeneration is a complex signaling process, an alternative pathway for protection by MY might also be involved. For instance, methylene blue is known to interact with the NMDA/iNOS pathway and thereby provide neuroprotection.[38] Future work will focus on elucidating these alternative pathways for MY.

Conclusions

PD is a debilitating neurodegenerative disease with no current therapies that could prevent or reverse the progression of the disease. Small molecules with multifunctionality (decreasing ROS production through MAO-B inhibition as well as neuroprotective characteristics such as preventing DA loss or preventing MPP^+ generation) have been developed in order to mitigate toxicity leading to neuronal death. For this work, we evaluated the novel compound MY and demonstrated its abilities as a potential drug scaffold for MAO-B inhibition with neuroprotective properties on the basis of in vitro (i.e., BBB permeability, serum albumin binding, drug efflux/metabolism, and mitochondrial toxicity) and in vivo (i.e., MPTP Parkinsonian mouse model) studies.

Experimental Section

All reagents were purchased from commercial suppliers and used as received unless stated otherwise. Azobenzene ((*E*)-1,2-diphenyldiazene) and MY ((*E*)-*N*,*N*-dimethyl-4-(phenyldiazenyl)aniline) were purchased from Alfa Aesar and Sigma, respectively. Absorbance required for assays was recorded on either a Synergy 4 plate reader (BioTek, Winooski, VT) or a Nanodrop UV/Vis spectrophotometer (Thermo Fisher Scientific). Fluorescence was measured by using a BioTek Synergy 4 plate reader.

MAO enzyme assays: MAO enzyme inhibition assays were performed by using recombinant human enzyme (BD Genetest, San Jose, CA) as previously described, with minor modifications.[15] For the measurement of enzyme activity, kynuramine was employed as a substrate. As kynuramine is metabolized by MAO, it forms a fluorescent metabolite 4-hydroxyquinoline ($\lambda_{ex} = 310$ nm; $\lambda_{em} = 380$ nm). The buffer system used was a 0.1 M phosphate buffer

(pH 7.4). The MAO enzyme assays were carried out in a fluorescent 96-well plate. The final concentrations of MAO-A and MAO-B were 6 $\mu g\,mL^{-1}$ and 15 $\mu g\,mL^{-1}$, respectively. The final concentration of kynuramine was 40 μM for MAO-A or 20 μM for MAO-B. The compounds (10 mM stock solution in DMSO; less than 2% (*v*/*v*) final concentration of DMSO in the assay) were incubated with MAO and the substrate for 20 min, after which the reaction was quenched with the addition of 2 N NaOH. IC_{50} values were determined by using Prism 5 statistical software (http://www.graphpad.com) and calculated from one-site binding, by using eight different concentrations spanning five log units, each performed in duplicate. Data are reported as the mean ± SEM, with each drug screened in duplicate.

Molecular modeling: Docking studies were performed by using MOE 2011.10 (Chemical Computing Group; http://www.chemcomp.com). The protein structure (PDB ID: 2V5Z)[16b] of MAO-B was used in which (*S*)-(+)-2-[4-(fluorobenzyloxyamino)propionamide] was cocrystallized, and the gating residue Ile 199 was in the open position. The B chain of MAO-B was deleted, and docking was carried out by using only one of the MAO-B chains. Prior to docking, the protein was protonated at pH 7.4 to correlate with the enzyme experiments. The binding site was identified as the area where the cocrystallized ligand was located. As MOE recognized flavin adenine dinucleotide (FAD) as a part of the ligand set, we first designated the ligand (*S*)-(+)-2-[4-(fluorobenzyloxyamino)propionamide] as such so that MOE could use this to delineate the binding pocket in the docking run. Only the top-returned binding pose of the ligand was further evaluated.

Parallel artificial membrane permeability assay: PAMPA experiments were conducted according to previously reported protocols with slight modifications.[17] A solution of hexadecane in hexane (5%, *v*/*v*) was added to the donor plate containing a polycarbonate (3 μM) filter membrane and was allowed to sit at room temperature for 45 min until the hexane evaporated. A solution containing 5% DMSO in phosphate-buffered saline (PBS, pH 7.4) was introduced to each well of the donor plate (150 μL) and acceptor plate (300 μL). The compounds were added to the donor plate (500 μM final concentration), and the donor plate was placed on top of the acceptor plate to form a sandwich. The sandwich was incubated for 5 h at room temperature. Fluorescence spectra of the solutions in the acceptor plate were measured at $\lambda_{ex/em} = 360/570$ nm. Propranolol was used as a positive control, with a fluorescent signal at $\lambda_{ex/em} = 300/338$ nm. Each drug was tested in triplicate wells.

Michaelis–Menten enzyme kinetics: The activity of MAO-B was evaluated in the absence and presence of inhibitor ([inhibitor] = 100, 200, 300, and 400 nM). The enzyme reaction was performed as mentioned before in a 96-well plate format, with the fluorescence detected as described previously.[11]

Reversibility study: To determine whether the type of enzyme inhibition was reversible or irreversible, MAO-B was preincubated with MY (50 nM) for set time points (0, 15, 30, 45, and 60 min), at which time kynuramine was added to start the reaction. The enzyme reaction was then terminated after 20 min, and the fluorescence intensity was measured as described previously. This assay was performed in a 96-well black plate (each bar represents $N = 8$ wells).

Serum albumin binding: Binding of MY to serum albumin was determined by using bovine serum albumin (BSA) as described previously.[17a,18] Briefly, MY (10 mM stock solution in DMSO) was serially diluted in a black 96-well plate to give an eight-point data curve. BSA was added to each well at a final concentration of 7.5 μM. Fluorescence quenching was analyzed at $\lambda_{ex/em} = 280/340$ nm. Each data point was done in triplicate wells.

Metabolism: P450 metabolic studies employing crude liver microsomes were carried out as previously described.[19] Mouse livers (C57BL6/J; Harlan Labs) were perfused with cold PBS (10 mL, pH 7.4) prior to blood removal. The livers were sliced into smaller pieces and placed into a Potter homogenizer on ice. Cold Tris buffer (100 mM, pH 7.4) was added at a volume three times that of the volume of tissues and homogenized with a Teflon-tipped pestle (ten strokes). The tissue homogenate was then centrifuged for 15 min (4 °C, 12000 *g*). The fatty layer was carefully removed, and the supernatant was saved for the metabolic studies. The protein concentration was determined by measuring absorbance (A_{280}) and adjusted to a final concentration of 2 $mg\,mL^{-1}$. The P450 metabolism assay with liver microsomes was modified to a 96-well black plate format, conducted in triplicate. Three different concentrations of the drug were diluted in Tris buffer (100 mM, pH 7.4), and an NADPH solution (10 mM) was added to give a final NADPH concentration of 2 mM. The reaction was initiated upon the addition of the microsomes to give a final concentration of 0.5 $mg\,mL^{-1}$ per well. After incubation for 1 h at 37 °C, fluorescence intensity was analyzed at $\lambda_{ex/em} = 340/450$ nm.

P-glycoprotein (P-gp) ATPase assay: A P-gp ATPase assay was conducted according to a previously published method by using recombinant protein, with minor modifications.[22] Recombinant human P-gp expressed in insect cells was purchased (BD Genetest) for membrane preparation. To test the activity of P-gp ATPase, a solution of drug or vehicle (DMSO) was treated with the membrane preparation (total of 40 μg protein) in a white clear-bottom 96-well plate, with each experiment performed in triplicate. Verapamil, a known substrate of P-gp, was used as a positive control (20 μM final concentration). The ATPase reaction was initiated with the addition of reaction buffer (50 mM Tris·MES, 2 mM EDTA, 50 mM KCl, 2 mM dithiothreitol, 5 mM sodium azide, and 2 μM MgATP, pH 6.8) and incubated in an Eppendorf 96-well plate heater/shaker for 30 min at 37 °C. The reaction was terminated with the addition of 100 μL of a Kinase-Glo solution (Promega). After incubation for 30 min at room temperature, luminescent signal was detected by using a Synergy 4 plate reader (BioTek). All experiments were carried out in triplicate.

Mitochondrial polarization assay: HTS detection of mitochondrial toxins was adapted from a previously published method.[24] A murine neuro-2a (N2a) neuroblastoma cell line was purchased from ATCC. The N2a cell line was cultured in Dulbecco's modified Eagle's medium (DMEM, Lonza, Walkersville, MD) supplemented with 10% fetal bovine serum (ATCC), penicillin (100 units mL^{-1}, Invitrogen), and streptomycin (100 $\mu g\,mL^{-1}$; Hyclone, Logan, UT). The cells were grown and maintained at 37 °C with 5% CO_2. The cells (50000 cells per well) were seeded into a 96-well black clear-bottom plate and allowed to adhere overnight. The medium was removed, and a solution containing either MY or trifluorocarbonylcyanide phenylhydrazone (FCCP, 50 μL, various concentrations) was added to each well, triplicate wells were used for each group. Tetramethylrhodamine methyl ester (TMRM) was added to each well at a final concentration of 50 nM. The plates were incubated for 30 min at 37 °C. After incubation, a brilliant black solution (15 $mg\,mL^{-1}$, 20 μL) was added, and fluorescence was detected ($\lambda_{ex} = 540/535$ nm; $\lambda_{em} = 620/640$ nm).

Western blot: Brain tissue samples were homogenized in cold lysis buffer (tenfold wet weight) containing protease inhibitors and phenylmethanesulfonylfluoride (PMSF). Homogenized brain tissue was

centrifuged for 15 min (14000 *g*, 4 °C). Protein in the supernatant was quantified by using a Pierce BCA protein assay kit (Thermo Scientific). Each sample containing 10 μg of protein was separated by using a 4–12% Bio-Rad miniProtean precast gel (200 V, 35 min). The protein was transferred onto a PVDF membrane (100 V, 1 h) and blocked for 1 h with 5% nonfat dry milk blocking solution in 0.2% TBST. The membrane was treated with a rabbit polyclonal anti-TH antibody (1:1000, Millipore) in TBST overnight at 4 °C and probed with a horseradish peroxidase-conjugated anti-rabbit secondary antibody (1:3000, Invitrogen) in TBST for 1 h. Each blot was then exposed to the Pierce ECL substrate and read on a Protein M chemiluminescent detector (http://www.proteinsimple.com).

Brain distribution: C57BL/6 mice were injected with MY (1 mg mg^{-1}) and, after 1 h, the brain was removed after a short (30 s) perfusion with PBS pH 7.4 to remove any residual drug from the brain vasculature. The brains were weighed, and three volumes of PBS were added. The tissue was homogenized by using a Dounce tissue homogenizer (pestles A and B), with at least four strokes each. Acetonitrile (CH_3CN) was then added, and the samples were mixed by vortexing. The samples were centrifuged for 10 min (10000 *g*, 4 °C). The CH_3CN fraction was used for HPLC analysis. A PerkinElmer HPLC was used, with a Thermo Hypersil-Keystone BioBasic-C18 column (5 μm 250×4.6 mm), and the column temperature set at 20 °C. The mobile phase consisted of 75% CH_3CN/25% H_2O, and the flow rate was 1 mL min^{-1}. The detection wavelength was set at 305 nm. An isocratic gradient was used. Four mice were used for the determination of brain distribution.

Neurochemical assay: Adult male C57BL/6 retired breeder mice were housed individually, had free access to food and water, and were maintained under a 12 h light cycle with lights on at 06:00. All treatments complied with the NIH guide for Care and Treatment of Laboratory Animals and were approved by the IACUC at NEOMED. All efforts were made to minimize animal suffering, to reduce the number of animals used, and to utilize alternatives to in vivo techniques when possible. Mice were treated with either 1) vehicle control (DMSO), 2) MPTP (35 mg kg^{-1} interperitoneal (i.p.) injection), 3) MPTP (35 mg kg^{-1} i.p.) and MY (1 mg kg^{-1} i.p.), or 4) MY (1 mg kg^{-1}. i.p.). MY was given 30 min before MPTP treatments. MY was dissolved in DMSO and injected at 1 μL g of mouse. At day 7 post-MPTP treatment, the brain was dissected to remove the striatum for HPLC analysis of DA content. For determinations of striatal tissue levels of DA, the tissue was weighed and placed in cold $HClO_4$ (0.1 N, 500 μL, 4 °C). These tissue samples were sonicated and centrifuged; an aliquot was removed to measure DA and 3,4-dihydroxyphenylacetic acid (DOPAC). Tissue samples were evaluated for DA content by HPLC with electrochemical detection. Biogenic amines were separated on a Supelco column (Discovery C18, 10 cm×3 mm×5 μm). Samples were injected into a 20 μL loop. A degassed isogradient mobile phase consisting of sodium acetate (50 mM), citric acid (27.4 mM), NaOH (10 mM), sodium octyl sulfate (0.1 mM), EDTA (0.1 mM), and 5% MeOH in filtered deionized water was used for the system. The mobile phase was adjusted to a final pH of 4.5 with the addition of NaOH and filtered (0.45 μm, Millipore filter) prior to use. Standards were diluted in perchloric acid (0.1 N) in increments of 3.1, 6.2, 12.5, 25, 50, 100, 200, and 400 pg/20 μL. Samples were analyzed by using the ESA 501 program. The assay sensitivity (6.2–12.5 pg/20 μL) was determined by the observation of reliable peaks above baseline noise.

Statistical analysis: Statistical analysis was performed by using a one-way ANOVA and Tukey's post-hoc test with InStat (Graphpad) statistical software. Statistical significance was considered when $p < 0.05$. Data are shown here as mean ± SEM, where the number of animals was four to five per treatment group.

Acknowledgements

This study was supported in part by the Ruth K. Broad Biomedical Foundation, the DGIST R&D Program of the Ministry of Science, ICT, and Future Planning of Korea (14-BD-0403), and the 2013 Research Fund of UNIST (project number 1.130068.01 to M.H.L.)

Keywords: MAO-B inhibitor · methyl yellow · MPTP mouse model · Parkinson's disease · TMRM

[1] S. von Campenhausen, B. Bornschein, R. Wick, K. Bötzel, C. Sampaio, W. Poewe, W. Oertel, U. Siebert, K. Berger, R. Dodel, *Eur. Neuropsychopharmacol.* **2005**, *15*, 473–490.
[2] a) C. M. Tanner, R. Ottman, S. M. Goldman, J. Ellenberg, P. Chan, R. Mayeux, J. W. Langston, *JAMA J. Am. Med. Assoc.* **1999**, *281*, 341–346; b) L. M. de Lau, M. M. Breteler, *Lancet Neurol.* **2006**, *5*, 525–535.
[3] C. A. Davie, *Br. Med. Bull.* **2008**, *86*, 109–127.
[4] D. Aarsland, S. Påhlhagen, C. G. Ballard, U. Ehrt, P. Svenningsson, *Nat. Rev. Neurol.* **2012**, *8*, 35–47.
[5] a) D. J. Karen, W. Li, P. R. Harp, J. S. Gillette, J. R. Bloomquist, *Neurotoxicology* **2001**, *22*, 811–817; b) J. M. Shulman, P. L. De Jager, M. B. Feany, *Annu. Rev. Pathol. Mech. Dis.* **2011**, *6*, 193–222; c) M. van der Mark, M. Brouwer, H. Kromhout, P. Nijssen, A. Huss, R. Vermeulen, *Environ. Health Perspect.* **2011**, *120*, 340–347.
[6] a) G. Cohen, R. Farooqui, N. Kesler, *Proc. Natl. Acad. Sci. USA* **1997**, *94*, 4890–4894; b) T. Nagatsu, M. Sawada, *J. Neural Transm. Suppl.* **2006**, *71*, 53–65; c) G. Lenaz, *Adv. Exp. Med. Biol.* **2012**, *942*, 93–136.
[7] a) P. Tuite, J. Riss, *Expert Opin. Invest. Drugs* **2003**, *12*, 1335–1352; b) M. B. Youdim, D. Edmondson, K. F. Tipton, *Nat. Rev. Neurosci.* **2006**, *7*, 295–309.
[8] C. Singer, *Cleveland Clin. J. Med.* **2012**, *79*, S3–S7.
[9] a) M. Löhle, H. Reichmann, *BMC Neurol.* **2011**, *11*, 112; b) P. Riederer, G. Laux, *Exp. Neurobiol.* **2011**, *20*, 1–17.
[10] C. J. Van der Schyf, S. Gal, W. J. Geldenhuys, M. B. Youdim, *Expert Opin. Invest. Drugs* **2006**, *15*, 873–886.
[11] W. J. Geldenhuys, K. S. Ko, H. Stinnett, C. J. Van der Schyf, M. H. Lim, *MedChemComm* **2011**, *2*, 1099–1103.
[12] A. Ferretta, A. Gaballo, P. Tanzarella, C. Piccoli, N. Capitanio, B. Nico, T. Annese, M. Di Paola, C. Dell'aquila, M. De Mari, E. Ferranini, V. Bonifati, C. Pacelli, T. Cocco, *Biochim. Biophys. Acta Mol. Basis Dis.* **2014**, *1842*, 902–915.
[13] a) J. Long, H. Gao, L. Sun, J. Liu, X. Zhao-Wilson, *Rejuvenation Res.* **2009**, *12*, 321–331; b) F. Jin, Q. Wu, Y. F. Lu, Q. H. Gong, J. S. Shi, *Eur. J. Pharmacol.* **2008**, *600*, 78–82; c) K. T. Lu, M. C. Ko, B. Y. Chen, J. C. Huang, C. W. Hsieh, M. C. Lee, R. Y. Chiou, B. S. Wung, C. H. Peng, Y. L. Yang, *J. Agric. Food Chem.* **2008**, *56*, 6910–6913.
[14] W. J. Geldenhuys, A. Bishayee, A. S. Darvesh, R. T. Carroll, *Curr. Pharm. Biotechnol.* **2012**, *13*, 117–124.
[15] W. J. Geldenhuys, A. S. Darvesh, M. O. Funk, C. J. Van der Schyf, R. T. Carroll, *Bioorg. Med. Chem. Lett.* **2010**, *20*, 5295–5298.
[16] a) F. Hubálek, C. Binda, M. Li, Y. Herzig, J. Sterling, M. B. Youdim, A. Mattevi, D. E. Edmondson, *J. Med. Chem.* **2004**, *47*, 1760–1766; b) C. Binda, J. Wang, L. Pisani, C. Caccia, A. Carotti, P. Salvati, D. E. Edmondson, A. Mattevi, *J. Med. Chem.* **2007**, *50*, 5848–5852.
[17] a) O. B. Al-Baghdadi, N. I. Prater, C. J. Van der Schyf, W. J. Geldenhuys, *Bioorg. Med. Chem. Lett.* **2012**, *22*, 7183–7188; b) F. Wohnsland, B. Faller, *J. Med. Chem.* **2001**, *44*, 923–930.
[18] A. Sułkowska, *J. Mol. Struct.* **2002**, *614*, 227–232.
[19] a) A. D. Rodrigues, D. J. Mulford, R. D. Lee, B. W. Surber, M. J. Kukulka, J. L. Ferrero, S. B. Thomas, M. S. Shet, R. W. Estabrook, *Drug Metab. Dispos.* **1995**, *23*, 765–775; b) V. C. Pillai, R. Mehvar, *J. Pharm. Sci.* **2011**, *100*, 3495–3505.
[20] D. Ouellet, C. Bramson, D. Roman, A. E. Remmers, E. Randinitis, A. Milton, M. Gardner, *Br. J. Clin. Pharmacol.* **2007**, *63*, 59–66.

[21] a) F. J. Sharom, *Essays Biochem.* **2011**, *50*, 161 – 178; b) G. N. Chan, R. Bendayan in *Methods in Molecular Biology, Vol. 686: Molecular and Functional Characterization of P-Glycoprotein in Vitro* (Ed.: S. Nag), Humana, Totowa, **2011**, 313 – 336.
[22] R. T. Carroll, D. Bhatia, W. Geldenhuys, R. Bhatia, N. Miladore, A. Bishayee, V. Sutariya, *J. Drug Targeting* **2010**, *18*, 665 – 674.
[23] M. Bauer, M. Zeitlinger, R. Karch, P. Matzneller, J. Stanek, W. Jäger, M. Böhmdorfer, W. Wadsak, M. Mitterhauser, J. P. Bankstahl, W. Löscher, M. Koepp, C. Kuntner, M. Müller, O. Langer, *Clin. Pharmacol. Ther.* **2012**, *91*, 227 – 233.
[24] A. Vongs, K. J. Solly, L. Kiss, D. J. Macneil, C. I. Rosenblum, *Assay Drug Dev. Technol.* **2011**, *9*, 373 – 381.
[25] H. Terada, *Environ. Health Perspect.* **1990**, *87*, 213 – 218.
[26] a) K. F. Tipton, T. P. Singer, *J. Neurochem.* **1993**, *61*, 1191 – 1206; b) N. Schmidt, B. Ferger, *J. Neural Transm.* **2001**, *108*, 1263 – 1282.
[27] J. A. Baur, Z. Ungvari, R. K. Minor, D. G. Le Couteur, R. de Cabo, *Nat. Rev. Drug Discovery* **2012**, *11*, 443 – 461.
[28] T. Herraiz, H. Guillen, *Food Chem. Toxicol.* **2011**, *49*, 1773 – 1781.
[29] a) C. Binda, M. Aldeco, W. J. Geldenhuys, M. Tortorici, A. Mattevi, D. E. Edmondson, *ACS Med. Chem. Lett.* **2012**, *3*, 39 – 42; b) C. Binda, A. Mattevi, D. E. Edmondson, *Int. Rev. Neurobiol.* **2011**, *100*, 1 – 11.
[30] G. F. Oxenkrug, S. O. Sablin, P. J. Requintina, *Ann. N. Y. Acad. Sci.* **2007**, *1122*, 245 – 252.
[31] A. Petzer, B. H. Harvey, G. Wegener, J. P. Petzer, *Toxicol. Appl. Pharmacol.* **2012**, *258*, 403 – 409.
[32] C. Dagenais, A. Avdeef, O. Tsinman, A. Dudley, R. Beliveau, *Eur. J. Pharm. Sci.* **2009**, *38*, 121 – 137.
[33] W. M. Pardridge, *Drug Discovery Today* **2007**, *12*, 54 – 61.
[34] M. Ingelman-Sundberg, *Toxicol. Appl. Pharmacol.* **2005**, *207*, 52 – 56.
[35] A. Camilleri, N. Vassallo, *CNS Neurosci. Ther.* **2014**, *20*, 591 – 602.
[36] a) J. A. Javitch, R. J. D'Amato, S. M. Strittmatter, S. H. Snyder, *Proc. Natl. Acad. Sci. USA* **1985**, *82*, 2173 – 2177; b) M. Del Zompo, M. P. Piccardi, S. Ruiu, M. Quartu, G. L. Gessa, A. Vaccari, *Br. J. Pharmacol.* **1993**, *109*, 411 – 414.
[37] a) T. Nagatsu, M. Levitt, S. Udenfriend, *J. Biol. Chem.* **1964**, *239*, 2910 – 2917; b) A. Petithomme Feve, *CNS Neurol. Disord. Drug Targets* **2012**, *11*, 450 – 455.
[38] A. Lomniczi, E. Cebral, G. Canteros, S. M. McCann, V. Rettori, *NeuroImmunoModulation* **2000**, *8*, 122 – 127.
[39] a) C. Binda, M. Aldeco, A. Mattevi, D. E. Edmondson, *J. Med. Chem.* **2011**, *54*, 909 – 912; b) P. K. Sonsalla, L. Y. Wong, B. Winnik, B. Buckley, *Exp. Neurol.* **2010**, *221*, 329 – 334.

Received: December 10, 2013
Revised: April 22, 2014
Published online on July 8, 2014